THE JOURNAL OF PHYSICAL CHEMISTRY B

ARTICLE

pubs.acs.org/JPCB

An Optimized Relaxation-Based Coherence Transfer NMR Experiment for the Measurement of Side-Chain Order in Methyl-Protonated, Highly Deuterated Proteins

Hechao Sun,[†] Lewis E. Kay,[‡,§] and Vitali Tugarinov*[,†]

[†]Department of Chemistry and Biochemistry, Center for Biomolecular Structure and Organization, University of Maryland, College Park, Maryland 20742, United States

[‡]Departments of Molecular Genetics, Biochemistry and Chemistry, University of Toronto, Toronto, Ontario, Canada M5S 1A8

[§]Hospital for the Sick Children, Program in Molecular Structure and Function, 555 University Avenue, Toronto, Ontario, Canada M5G 1X8

ABSTRACT:

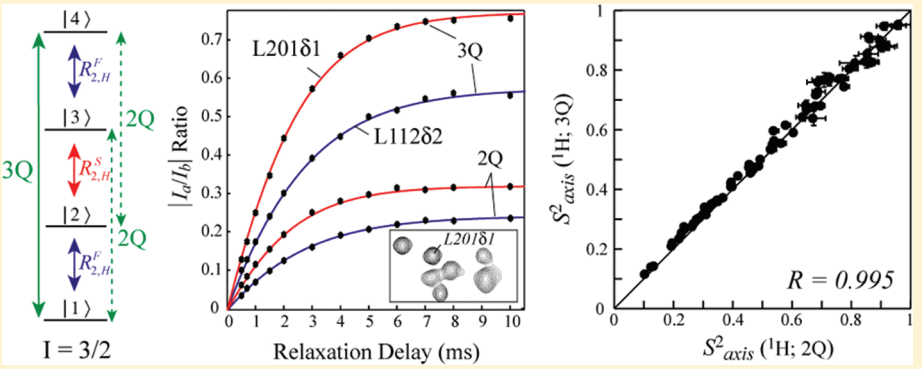

Relaxation violated coherence transfer NMR spectroscopy has emerged as a powerful experimental tool for the quantitative measurement of amplitudes of motion of methyl containing side-chains. Typically, the experiments, performed on proteins that are highly deuterated and methyl-protonated, monitor the build-up of methyl ^{1}H double-quantum magnetization. Because all three protons in a methyl group are degenerate, such coherences can only result from differential relaxation of transverse magnetization components, which in turn reflect the extent and time-scale of motion of the methyl probe [Tugarinov, V., Sprangers, R.; Kay, L.E. *J. Am. Chem. Soc.* **2007**, *129*, 1743−1750]. We show here that a 50% gain in the sensitivity of the experiment can be achieved through selection of ^{1}H triple-quantum coherence, thereby significantly increasing the utility of the approach. A theoretical treatment rationalizes the sensitivity gain that is subsequently verified through experiment. The utility of the methodology is demonstrated on a number of proteins, including the 360 kDa $\alpha_7\alpha_7$ "half-proteasome".

INTRODUCTION

Methyl groups have emerged as important probes in NMR studies of both protein structure and dynamics.[1−6] Initial methyl relaxation experiments, dating back to the pioneering studies from the laboratories of Wüthrich,[7] Gurd,[8] and Sykes,[9] were based on ^{13}C one-dimensional spectroscopy and were performed on concentrated protein samples. In the intervening three decades, the advent of multidimensional NMR spectroscopy[10−14] and the development of new labeling schemes[4,15−17] have led to a significant increase in the range of protein systems that can be investigated and the types of experiments that can be performed.[18,19] It is now possible to quantify the mobility of methyl containing side-chains through the use of ^{2}H, ^{13}C and ^{1}H spin relaxation experiments that are specifically tailored to the labeling approach that is used.[3,6,20] For example, deuterium spin relaxation experiments have been developed for measuring the decay of longitudinal and in-phase transverse magnetization as well as antiphase transverse, quadrupole order, and double quantum terms using $^{13}CH_2D$[21−23] or $^{13}CHD_2$[23,24] methyl groups. These experiments are powerful because the quadrupolar interaction dominates to the point that other relaxation mechanisms, such as those that are dipolar in origin, can be safely ignored.[21−23,25] ^{13}C methyl spin relaxation experiments have in turn exploited the "two deuterons, one proton" labeling pattern[26−30] ($^{13}CHD_2$), which eliminates undesired ^{13}C−^{1}H dipole−dipole cross-correlated relaxation effects that would otherwise complicate interpretation of ^{13}C relaxation in $^{13}CH_3$ methyl groups.[31,32] Comprehensive accounts of cross-correlated spin relaxation in methyl groups can be found in papers by Werbelow and Grant[33] and Vold and Vold.[34] In the case of ^{13}C studies involving $^{13}CHD_2$ methyls, the

Received: September 19, 2011
Revised: October 30, 2011
Published: October 31, 2011

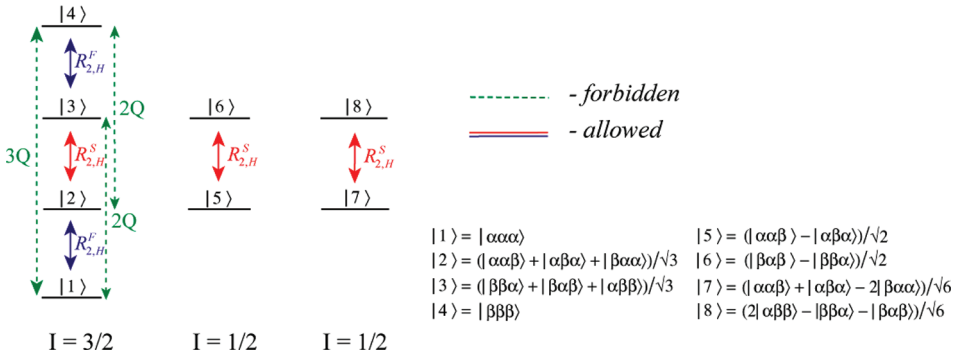

Figure 1. Energy level diagram for the X_3 spin-system of a (C)H_3 methyl group. Slow(fast)-relaxing allowed transitions are shown with red(blue) solid arrows and labeled as $R^S_{2,H}(R^F_{2,H})$. Multiple-quantum (forbidden) proton transitions are shown with green dashed arrows. The ^{1}H eigenstates are depicted by $|i,j,k\rangle$ $(i,j,k \in \{\alpha,\beta\})$.

relaxation of interest arises mainly from intramethyl ^{13}C−^{1}H and ^{13}C−^{2}H dipolar contributions and to a much smaller extent from hydrogens at positions adjacent to the methyl of interest.[27,28] Although interpretation of the relaxation data is thus necessarily less straightforward than for deuterium, an advantage is the considerably improved sensitivity (generally 3−5 fold).[28−30,35]

Additional approaches for quantifying motion in methyl containing side-chains have emerged in the past several years that exploit methyl ^{1}H spin-relaxation in highly deuterated proteins.[6,36,37] These include the measurement of transverse relaxation rates of individual methyl ^{1}H transitions.[36] Alternatively, a more sensitive approach relies upon the measurement of ^{1}H−^{1}H dipolar cross-correlation rates, η, using coherence transfer via relaxation,[11,38,39] whereby methyl proton double-quantum (2Q) (or so-called "forbidden") coherences are created within a spin-system where all the methyl protons are magnetically equivalent.[37] Our interest in using intramethyl ^{1}H−^{1}H dipolar relaxation to probe dynamics in proteins is somewhat pragmatic. Studies of high-molecular-weight proteins most often begin with a highly deuterated, $^{13}CH_3$-methyl labeled sample (typically involving Ile $C^{\delta 1}$, Leu C^{δ}, and Val C^{γ} moieties).[16,29,40,41] Exploiting this labeling scheme in as many ways as possible is thus both efficient and cost-effective, and indeed in recent years the forbidden 2Q relaxation experiment has been applied to a number of large protein assemblies.[3,29,42,43] Recent studies have shown that consistent measures of side-chain order are obtained from methyl ^{1}H, ^{13}C, and ^{2}H experiments, although in the case of ^{1}H relaxation studies a requirement for proteins with tumbling times on the order of ∼10 ns or larger (slow tumbling limit) has been noted.[36,37]

Because of the importance of the $^{13}CH_3$ methyl probe in relaxation studies, we have revisited some of our earlier experiments[37] in the hope of developing new approaches that offer significant improvements in sensitivity. We find that a scheme exploiting the creation of methyl ^{1}H triple-quantum (3Q) coherence from ^{1}H−^{1}H dipolar cross-correlated spin relaxation is 50% more sensitive than the corresponding 2Q-based experiment. Interestingly, such sensitivity gains are in direct contrast to expectations based on the relative efficiencies of excitation of 2Q and 3Q coherences in an AMX spin system resulting from evolution due to scalar couplings where the sensitivity of the pQ data set scales as 2^{-p}.[11,44] The predicted sensitivity gain is verified experimentally on a number of protein systems including 82 kDa malate synthase G (MSG),[18,45] highly deuterated and labeled with $^{13}CH_3$ groups at Ile$^{\delta 1}$ methyl positions and a highly deuterated 360 kDa $\alpha_7\alpha_7$ "half-proteasome" sample[29] labeled with $^{13}CH_3$ methyls at Ile$^{\delta 1}$, Leu$^{\delta}$, and Val$^{\gamma}$ methyl sites. The utility of dynamics measurements using the forbidden 3Q scheme reported here is established by cross-validation of the extracted methyl axis order parameters with those obtained from other more established experiments.

MATERIALS AND METHODS

NMR Samples. Several protein systems have been used in this study, including (i) {U-[^{15}N,^{2}H]; Ile$^{\delta 1}$-[$^{13}CH_3$]; Leu,Val-[$^{13}CH_3$,$^{12}CD_3$]}-labeled B1 immunoglobulin binding domain of peptostreptoccocal protein L (7.5 kDa), (ii) {U-[^{15}N,^{2}H]; Ile$^{\delta 1}$-[$^{13}CH_3$]; Leu,Val-[$^{13}CH_3$,$^{12}CD_3$]}-labeled human ubiquitin (8.5 kDa), (iii) {U-[^{15}N,^{2}H]; Ile$^{\delta 1}$-[$^{13}CH_3$]} MSG (82 kDa), and (iv) {U-[^{15}N,^{2}H]; Ile$^{\delta 1}$-[$^{13}CH_3$]; Leu,Val-[$^{13}CH_3$,$^{12}CD_3$]}-labeled half-proteasome $\alpha_7\alpha_7$ (360 kDa). All samples were prepared as described in detail previously[29,46−48] using [U−^{2}H]-glucose as the main carbon source and the appropriate α-keto-acid precursors for selective methyl labeling.[16,49] Sample conditions were 1.4 mM protein L, 99.9% D_2O, 50 mM sodium phosphate, pH 6.0 (uncorrected); 1.2 mM ubiquitin, 99.9% D_2O, 25 mM sodium phosphate, pH 6.8 (uncorrected), 0.05% NaN_3; 0.5 mM MSG, 99.9% D_2O, 25 mM sodium phosphate, pH 7.1 (uncorrected), 20 mM $MgCl_2$, 0.05% NaN_3, 5 mM DTT; 0.14 mM $\alpha_7\alpha_7$ (concentration of complex), 99.9% D_2O, 25 mM potassium phosphate, pH 6.8 (uncorrected), 50 mM NaCl, 1 mM EDTA, 0.03% NaN_3 and 2 mM DTT.

NMR Experiments and Data Analysis. Experiments on protein L (5 °C) and $\alpha_7\alpha_7$ half-proteasome (50 °C) were performed on an 800 MHz Varian Inova spectrometer equipped with a room-temperature probehead, while NMR measurements on ubiquitin (10 °C) and MSG (37 °C) were carried out at 600 MHz using a Bruker Avance III spectrometer with a room-temperature triple-resonance probe. All NMR spectra were processed and analyzed using the NMRPipe/NMRDraw suite of programs and associated software.[50] Intramethyl ^{1}H−^{1}H dipolar cross-correlated relaxation rates η have been obtained by fitting ratios of peak intensities measured in pairs of data sets recorded as a function of relaxation time, T, (see Figure 2 below and Figure 3 of Tugarinov et al.[37]) to the equation described in the text. Errors in the extracted values of η were generated by a Monte Carlo analysis[51] using random noise in the spectra as an estimate of experimental uncertainties in peak intensities.

The time dependencies of peak intensities in the η cross-correlation rate measurements (for both forbidden 2Q and 3Q experiments)

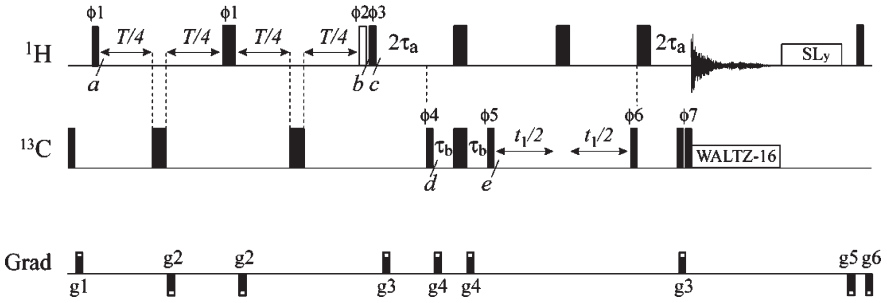

Figure 2. Optimized pulse scheme for the measurement of intramethyl ^{1}H−^{1}H dipolar cross-correlated relaxation rates, $\eta = (R^F_{2,H} - R^S_{2,H})/2$, with selection of forbidden 3Q transitions. The scheme with the open ^{1}H pulse included at point *b* is used to measure the build-up of 3Q coherences during the relaxation delay *T* (resulting in correlations with intensities I_a), while a second experiment is recorded to measure the biexponential decay of ^{1}H SQ magnetization by removing the open pulse (correlations with intensities I_b). All narrow(wide) rectangular pulses are applied with flip angles of 90(180)° along the *x*-axis unless indicated otherwise. The ^{1}H carrier is positioned in the center of the Ile$^{\delta1}$-Leu-Val methyl region, 0.7 ppm, while the ^{13}C carrier is positioned at 12(19) ppm for Ile$^{\delta1}$(ILV)-labeled samples. All ^{1}H and ^{13}C pulses are applied with the highest possible power, with WALTZ-16[59] ^{13}C decoupling achieved using a 2 kHz field. A 40 ms ^{1}H spin-lock field (10 kHz, *y*-axis) is applied after acquisition ('SLy'). This "SLy" and the subsequent ^{1}H purge eliminates all transverse components of magnetization. Delays are $\tau_a = 1/(4^1J_{CH}) = 2.0$ ms; $\tau_b = 1/(8^1J_{CH}) = 1$ ms; *T* is a variable relaxation delay. The phase cycle is ϕ1 = (0°,60°,120°,180°,240°,300°); ϕ2 = (ϕ1 + 90°); ϕ3 = 6(*y*),6(−*y*); ϕ4 = 12(*x*),12(−*x*); ϕ5 = 6(*y*),6(−*y*); ϕ6 = *x*; ϕ7 = 6(*x*),6(−*x*); rec. = 6(*x*,−*x*),6(−*x*,*x*) (3Q forbidden experiment), and ϕ1 = *x*,−*x*; ϕ3 = 2(*y*),2(−*y*); ϕ4 = 8(*x*),8(−*x*); ϕ5 = 4(*y*),4(−*y*); ϕ6 = *x*; ϕ7 = 8(*x*),8(−*x*); rec. = 4(*x*,−*x*),4(−*x*,*x*) (allowed experiment). The durations and strengths of pulsed-field *z*-gradients in units of (ms; G/cm) are g1 = (1; 40), g2 = (0.05; −20), g3 = (0.5; 20), g4 = (0.15; 12), g5 = (1.2; −24), g6 = (0.6; −24). Quadrature detection in F_1 is achieved via STATES-TPPI[60] of phase ϕ6. The phase cycle used for 2Q selection is ϕ1 = (*x*,*y*,−*x*,−*y*); ϕ2 = ϕ1; ϕ3 = 4(*x*),4(−*x*); ϕ4 = 8(*x*),8(−*x*); ϕ5 = 4(*y*),4(−*y*); ϕ6 = *x*; ϕ7 = 8(*x*),8(−*x*); rec. = 2(*x*,−*x*),4(−*x*,*x*),2(*x*,−*x*).[37] Note that *C* = 3/4 (3Q) and 1/2 (2Q) in eq 7 assumes that the same number of transients is recorded for the "a" and "b" experiments. Since $I_a < I_b$ additional scans are typically obtained for "a", in the case where N_a and N_b scans are recorded for experiments "a" and "b" then *C* must be multiplied by N_b/N_a prior to fitting the data with eq 7.

were monitored using the following sets of relaxation delays *T*: (2, 7, 12, 17, 22, 27, 32, 37, 42) ms for protein L at 5 °C, (4, 8, 12, 16, 20, 24, 28, 32, 37, 41, 44, 48) ms for ubiquitin at 10 °C, (0.8, 2, 3, 4, 6, 8, 10, 14) ms for MSG at 37 °C and (0.4, 0.7, 1, 1.5, 2, 3, 4, 5, 6, 7, 8, 10) ms for the $\alpha_7\alpha_7$ half-proteasome at 50 °C. All measurements were performed in an interleaved mode, whereby FIDs for the "allowed" data set (referred to in what follows as "b") and for the forbidden data set ("a") at a given value of the relaxation delay *T* and t_1 evolution time were recorded one after the other. Typically, recovery delays of 1.5 s and 24 scans/fid were employed resulting in net acquisition times of approximately 4 h for each pair of forbidden and allowed data sets.

Extraction of methyl 3-fold axis order parameters, S^2_{axis}, from relaxation data requires knowledge of the protein's overall molecular tumbling time (τ_C). A τ_C value of 10.2 ns (assumed isotropic) has been used for protein L in D_2O at 5 °C,[37,52] while the correlation time of ubiquitin (D_2O; 10 °C) determined previously in H_2O at 10 °C from ^{15}N relaxation data[53] has been scaled by the ratio of D_2O/H_2O viscosities,[54] $\tau_C(D_2O) = [\eta^{D2O}/\eta^{H2O}]\tau_C(H_2O) = 8.9$ ns (again assumed isotropic). The values of the diffusion tensor for MSG (D_2O; 37 °C) were estimated as described previously,[23,36] with $\tau_{C,eff} = (2D_{\|} + 4D_{\perp})^{-1} = 49$ ns, diffusion anisotropy $D_{\|}/D_{\perp} = 1.21$, and polar angles $\theta = 13°$, $\phi = 48°$ describing the orientation of the unique diffusion axis relative to the inertia frame. In the case of the $\alpha_7\alpha_7$ half-proteasome at 50 °C, an isotropic τ_C value of 109 ns was used in all calculations as in previous studies.[37]

RESULTS AND DISCUSSION

Creating 3Q ^{1}H Coherences in an X_3 Spin-System. Before describing the experimental scheme for extracting methyl S^2_{axis} values from the time-dependence of the build-up of forbidden 3Q ^{1}H coherences, we briefly summarize the basic features of an X_3 energy level diagram that are necessary for understanding the approach that we use. Further details have been provided in a previous publication.[37] Figure 1 shows the energy level diagram for a (C)H_3 methyl group. Although the ^{13}C spin is important for providing an "extra dimension" to resolve methyl groups in complex spectra and for exploiting a methyl-TROSY effect that improves the sensitivity of correlations in high-molecular-weight proteins via cross-correlated spin relaxation,[48] it is "not required" for the excitation of 3Q ^{1}H coherences and will therefore not be included in the discussion that follows. Assuming an "isolated" methyl group attached to a macromolecule with very rapid rotation about the methyl 3-fold axis, it has been shown that relaxation of each of the ^{1}H single-quantum (SQ) transitions occurs in a single-exponential manner, with fast ($R^F_{2,H}$, shown with blue arrows in Figure 1) or slow ($R^S_{2,H}$, red arrows) rates.[38,39,48] It has also been shown that differences in $R^F_{2,H}$ and $R^S_{2,H}$ derive from intramethyl ^{1}H−^{1}H dipolar cross-correlated relaxation with a rate, η, given by[37]

$$\eta = \frac{R^F_{2,H} - R^S_{2,H}}{2} \approx \frac{9}{10}\left(\frac{\mu_o}{4\pi}\right)^2 [P_2(\cos\theta_{axis,HH})]^2 \frac{S^2_{axis}\gamma^4_H\hbar^2\tau_c}{r^6_{HH}} \quad (1)$$

In eq 1, τ_C is the global molecular tumbling time, μ_0 is the vacuum permittivity constant, γ_H is the gyromagnetic ratio of a proton spin, r_{HH} is the distance between pairs of methyl protons (1.813 Å),[27,36] S_{axis} is the generalized order parameter describing the amplitude of motion of the methyl 3-fold axis, $P_2(x) = 1/2(3x^2 - 1)$, and $\theta_{axis,HH}$ is the angle between the methyl 3-fold axis and a vector connecting a pair of methyl ^{1}H nuclei.

Figure 2 shows the pulse scheme that has been derived to measure η and hence quantify S_{axis} values based on the creation of 3Q coherences. We initially concentrate on the portion of the sequence between points *a*−*c* that is the "business end" of the experiment using phases for the first three 90° ^{1}H pulses of ϕ1 = *y*, ϕ2 = *x*, and ϕ3 = *x* and retain only terms of interest that

ultimately contribute to the observed signal (i.e., that survive the complete phase cycle).

Transverse ^{1}H magnetization, created by the first 90° pulse at point *a* of the scheme, evolves for a period *T*. The differential relaxation of the fast and slowly relaxing components, corresponding to the blue and red transitions of Figure 1, respectively, facilitates the creation of 3Q coherences through the application of the second 90° pulse ("open", phase $\phi 2$)

$$\rho_b^{3Q} = \frac{3}{4}[\exp(-R_{2,H}^S T) - \exp(-R_{2,H}^F T)][|1\rangle\langle 4| + |4\rangle\langle 1|] \quad (2)$$

In eq 2, ρ_b^{3Q} is the density matrix that, for simplicity, includes only the 3Q transitions $|1\rangle\langle 4|$ and $|4\rangle\langle 1|$, where $|i\rangle\langle j|$ is a coherence connecting states $|i\rangle$ and $|j\rangle$ (see legend to Figure 1). Clearly in the limit that $R_{2,H}^F = R_{2,H}^S$, $\rho_b^{3Q} = 0$ and 3Q coherences cannot be created.

The remaining portion of the pulse scheme is effectively an HMQC[55,56] sequence with a "purge" element (between points *d* and *e*) that eliminates the rapidly relaxing ^{1}H−^{13}C multiple quantum coherences, so that only the slowly relaxing components are retained, as described previously.[37] Thus, immediately prior to acquisition, the density matrix of interest is given by

$$\rho^{SQ} = \frac{9}{16}[\exp(-R_{2,H}^S T) - \exp(-R_{2,H}^F T)]\cos(\omega_C t_1)[|2\rangle\langle 3| + |3\rangle\langle 2|] \quad (3)$$

where $|2\rangle\langle 3|$ and $|3\rangle\langle 2|$ are slowly relaxing ^{1}H SQ coherences (rate $R_{2,H}^S$), and ω_C is the Larmor frequency of the methyl ^{13}C spin of interest. Terms proportional to $\sin(\omega_C t_1)$ are also generated in subsequent scans so that quadrature in F_1 can be obtained. Thus, correlations are obtained at (ω_C, ω_H) with intensities, I_a,

$$I_a = A\frac{9}{8}[\exp(-R_{2,H}^S T) - \exp(-R_{2,H}^F T)] \quad (4)$$

where *A* is a constant that takes into account relaxation during τ_a, τ_b, t_1, and t_2. It is worth noting that only magnetization from the 3/2 manifold of Figure 1 is retained in the experiment because 3Q coherences cannot be excited from the two $I = 1/2$ manifolds.

In order to obtain η values, a second experiment is performed with the 90° ^{1}H pulse of phase ϕ_2 removed (referred to as experiment "b"). Only SQ coherences are of interest, including those from both $I = 3/2$ and $I = 1/2$ manifolds, and it has been shown previously[37] that in this case the intensities of correlations are given by

$$I_b = A\frac{3}{2}[\exp(-R_{2,H}^S T) + \exp(-R_{2,H}^F T)] \quad (5)$$

with the same constant of proportionality (*A*) as for I_a. It follows, therefore, that

$$\left|\frac{I_a}{I_b}\right| = \frac{3}{4}\tanh(\eta T) \quad (6)$$

and the values of η are obtained directly from ratios of peak intensities in the two experiments.

In the discussion above, we have assumed that the methyl group is isolated so that there are no relaxation contributions from external spins (i.e., protons on other methyl groups). This is of course not the case. Taking into account relaxation from external ^{1}H spins, as described in detail previously,[37] it has been shown that

$$\left|\frac{I_a}{I_b}\right| = C\frac{\eta\tanh(\sqrt{\eta^2 + \delta^2}T)}{\sqrt{\eta^2 + \delta^2} - \delta\tanh(\sqrt{\eta^2 + \delta^2}T)} \quad (7)$$

where $C = 3/4$ in this case and δ (<0) accounts for coupling between the rapidly and slowly decaying ^{1}H SQ coherences due to relaxation with external protons. In order to minimize the effects of external relaxation, it is advisible to work with highly deuterated proteins, with protonation confined only to methyl positions and with only one of the two isopropyl groups of Val and Leu residues protonated.[49]

Comparison of Forbidden 3Q and 2Q Experiments. A strong motivation for the present study was to develop an experiment with improved sensitivity relative to the 2Q scheme that we proposed several years earlier.[37] A calculation similar to that presented above has already been given for the ratio $|I_a/I_b|$ in the 2Q experiment, where eq 7 is obtained with $C = 1/2$.[37] Thus, while it is clear that the 3Q scheme is 1.5 fold more sensitive (and we demonstrate this experimentally below), it is of interest to understand from where the extra signal is derived.

The efficiency of excitation of 3Q ^{1}H coherences relative to 2Q ^{1}H coherences in an X_3 spin system can be calculated from eq 2 and the corresponding expression for the density matrix that considers the 2Q terms that was derived previously,[37]

$$\rho_b^{2Q} = \frac{\sqrt{3}}{4}[\exp(-R_{2,H}^F T) - \exp(-R_{2,H}^S T)][-|1\rangle\langle 3| - |3\rangle\langle 1| + |2\rangle\langle 4| + |4\rangle\langle 2|] \quad (8)$$

Note that both ρ_b^{3Q} and ρ_b^{2Q} are expanded over an orthogonal basis, $B_{ij} = |i\rangle\langle j|$, such that $\mathrm{Tr}\{B_{ij}B_{kl}^+\} = \delta_{ik}\delta_{jl}$, where "Tr" is the trace operator, "+" indicates transpose, and $\delta_{ab} = 1(0)$ if $a = b (a \neq b)$. Sørensen[57] has shown that the efficiency of a transfer step from a starting density matrix $\rho_{initial} = \Sigma_{i,j} b_{ij}^{initial} B_{ij}$ to a final state $\rho_{final} = \Sigma_{i,j} b_{ij}^{final} B_{ij}$, *E*, is then given by $E = (\|\rho_{final}\|)/(\|\rho_{initial}\|)$, where $(\|\rho\|) = (\Sigma_{i,j} b_{ij}^2)^{1/2}$. It can, therefore, be shown that

$$\frac{E^{SQ \rightarrow 3Q}}{E^{SQ \rightarrow 2Q}} = \frac{\left\|\rho_b^{3Q}\right\|}{\left\|\rho_b^{2Q}\right\|} = \sqrt{\frac{3}{2}} \quad (9)$$

so that excitation of 3Q coherences from the SQ density elements that evolve during *T* in Figure 2 is $(3/2)^{1/2}$ more efficient than the process of exciting 2Q coherences. In a similar manner, it is straightforward to show that the transfer from 3Q coherences to observable magnetization, corresponding to the slowly relaxing ^{1}H SQ coherences that derive from the 3/2 manifold (see Figure 1), is also more efficient than for 2Q in the sense that $E^{3Q \rightarrow SQ}/E^{2Q \rightarrow SQ} = (3/2)^{1/2}$. The net relative transfer efficiency is given by the product of the relative efficiencies over each of the two steps, SQ→*n*Q and *n*Q→SQ ($n = 2,3$),

$$\left(\frac{E^{SQ \rightarrow 3Q}}{E^{SQ \rightarrow 2Q}}\right)\left(\frac{E^{3Q \rightarrow SQ}}{E^{2Q \rightarrow SQ}}\right) = 1.5 \quad (10)$$

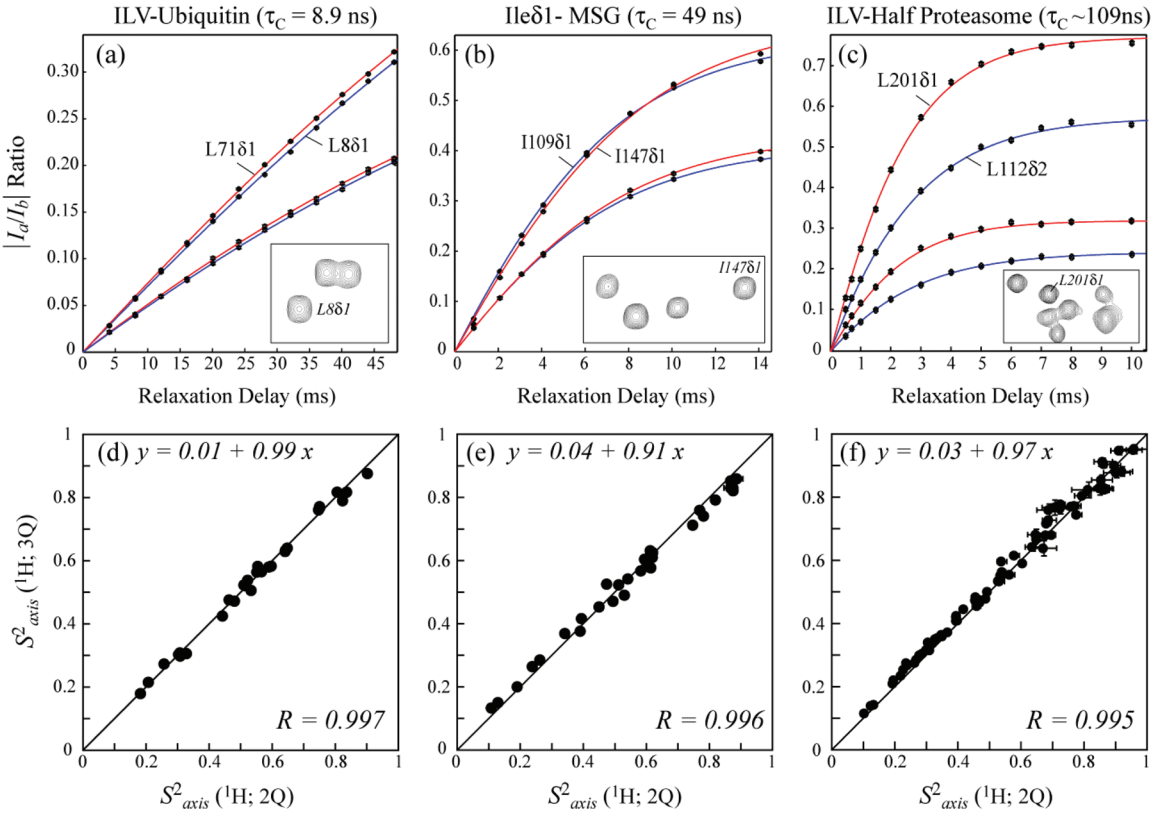

Figure 3. (a−c) Plots of experimental $|I_a/I_b|$ versus relaxation delay T, for selected residues from ubiquitin, MSG, and $\alpha_7\alpha_7$ as described in the text. Data from both 2Q and 3Q experiments are shown, with intensities I_a obtained from the 3Q(2Q) forbidden experiment in the upper(lower) curves. Shown also are best fits (solid lines) to eq 7 with C = 3/4 for 3Q and C = 1/2 for 2Q selection, normalized as appropriate to take into account different numbers of scans in the "a" and "b" experiments (see legend to Figure 2). (a) Leu8$^{\delta1}$ (blue) and Leu71$^{\delta1}$ (red) methyl groups of {U-[^{2}H;^{15}N]; Ile$^{\delta1}$-[^{13}CH$_3$]; Leu,Val-[^{13}CH$_3$,^{12}CD$_3$]}-ubiquitin (600 MHz; 10 °C). (b) Ile109$^{\delta1}$ (blue) and Ile147$^{\delta1}$ (red) methyls of {U-[^{2}H;^{15}N]; Ile$^{\delta1}$-[^{13}CH$_3$]}-MSG (600 MHz; 37 °C). (c) Leu112$^{\delta2}$ (blue) and Leu201$^{\delta1}$ (red) methyl groups of the {U-[^{2}H;^{15}N]; Ile$^{\delta1}$-[^{13}CH$_3$]; Leu,Val-[^{13}CH$_3$,^{12}CD$_3$]}-$\alpha_7\alpha_7$ half-proteasome (800 MHz; 50 °C). Insets show selected regions of spectra containing one of the two highlighted methyls. (d-f) Linear correlation plots of S^2_{axis} values obtained using the 3Q version of the forbidden experiment in Figure 2 (y-axis; ^{1}H 3Q) and the forbidden 2Q scheme (x-axis; ^{1}H 2Q). (d) ILV methyls of ubiquitin (29 peaks), (e) Ile$^{\delta1}$ methyls of MSG (30 peaks) and (f) ILV methyls of the $\alpha_7\alpha_7$ half-proteasome (74 peaks). Best-fit parameters from linear regression analyses of the data are shown along with Pearson correlation coefficients, R. Diagonal lines correspond to $y = x$.

that is, of course, consistent with the fact that C in eq 7 is 3/4 and 1/2 for the 3Q and 2Q experiments, respectively. Thus, the forbidden 3Q experiment is predicted to be 50% more sensitive than the corresponding 2Q analogue.

This predicted increase in sensitivity, verified in the subsequent section, is also observed in a comparison of 3Q versus 2Q spectra of an aligned spin-3/2 particle where the excitation of the multiple quantum coherence of interest derives from the nonzero quadrupolar splitting rather than from spin relaxation.[58] This is quite different from what is observed for an AMX spin system. Here, cross-peaks in a 2Q-filtered COSY experiment are 2-fold more intense than the corresponding correlations in a 3Q-filtered data set, with the intensity scaled, generally, in proportion to 2^{-p} where p is the coherence order.[11,44]

Experimental Verification. In order to establish that the 3Q-filtered experiment is 50% more sensitive than the corresponding 2Q scheme and to further illustrate the utility of the 3Q pulse scheme in studies of protein dynamics, we have recorded both 2Q and 3Q experiments on a variety of different protein systems ranging in correlation times from approximately 10 to 110 ns. Figure 3 plots experimental intensity ratios, $|I_a/I_b|$, as a function of relaxation delay T obtained from correlations in 3Q (upper curves) and 2Q data sets. In Figure 3a−c selected residues from {U-[^{2}H; ^{15}N]; Ile$^{\delta1}$-[^{13}CH$_3$]; Leu,Val-[^{13}CH$_3$,^{12}CD$_3$]}-ubiquitin (10 °C, 3a), {U-[^{2}H; ^{15}N]; Ile$^{\delta1}$-[^{13}CH$_3$]}-MSG (37 °C, 3b), and {U-[^{2}H; ^{15}N]; Ile$^{\delta1}$-[^{13}CH$_3$]; Leu,Val-[^{13}CH$_3$,^{12}CD$_3$]}-$\alpha_7\alpha_7$ half-proteasome (50 °C, 3c) are highlighted.

Figures 3a-c establish that the intensity ratios $|I_a(3Q)/I_b|$ are larger than $|I_a(2Q)/I_b|$, as expected from eq 10. Average values of $I_a(3Q)/I_a(2Q)$ are 1.48 ± 0.02, 1.49 ± 0.02, 1.48 ± 0.03 and 1.47 ± 0.05 for protein L, ubiquitin, MSG, and $\alpha_7\alpha_7$, respectively, in good agreement with the expected ratio of 1.5. Values of η have been extracted from fits of the experimental $|I_a/I_b|$ ratios to eq 7 with C = 3/4 (3Q) and 1/2 (2Q). Average η rates (±1 standard deviation) of 21 ± 7 (protein L), 20 ± 6 (ubiquitin), 107 ± 29 (MSG) and 232 ± 98 s^{-1} ($\alpha_7\alpha_7$) are fitted from the 3Q I_a/I_b profiles that are in good agreement with the corresponding set of rates, 22 ± 7, 20 ± 6, 105 ± 30, and 234 ± 101 s^{-1} obtained from the 2Q-filtered experiments.

S^2_{axis} values have been computed directly from η using eq 1 and values of τ_C listed in the Materials and Methods. Figure 3d−f shows that excellent correlations are obtained for S^2_{axis} values derived from data sets recorded using 3Q and 2Q versions of the forbidden experiment for ubiquitin, MSG, and $\alpha_7\alpha_7$, and correlations of very similar quality are obtained for protein L as well. In previous studies we have shown that there is excellent agreement

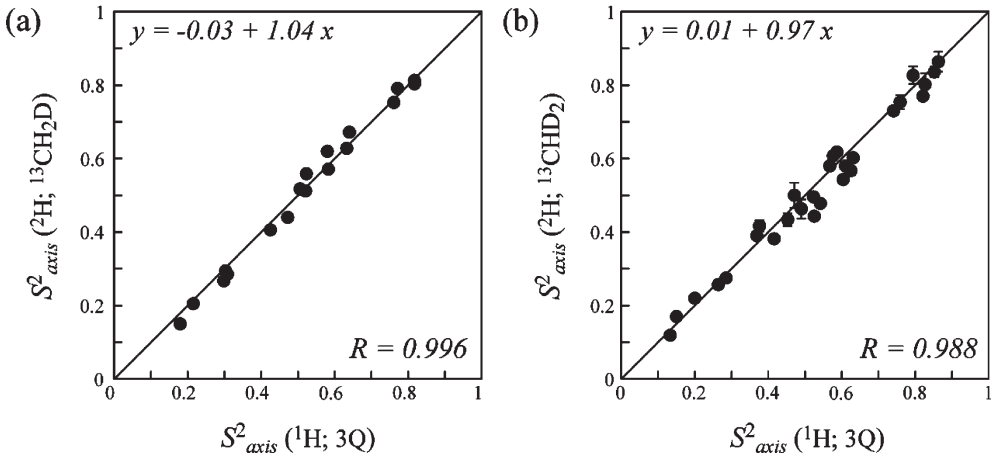

Figure 4. Linear correlation plots of ^{2}H-derived S^2_{axis} values (y-axis) versus S^2_{axis} obtained from extracted cross-correlation rates η measured using the forbidden 3Q experiment (x-axis; ^{1}H 3Q) for (a) 19 Leu$^{\delta}$, Val$^{\gamma}$ methyl groups ($^{13}CH_2D$) of ubiquitin (10 °C), and (b) 30 Ile$^{\delta 1}$ methyls ($^{13}CHD_2$) of MSG (37 °C). Best-fit parameters from a linear regression analysis of the data are shown for each plot along with Pearson correlation coefficients, R. Diagonal lines correspond to $y = x$.

between order parameters obtained from the 2Q ^{1}H-based relaxation experiment and experiments exploiting either ^{13}C or ^{2}H spin relaxation.[36,37] The excellent agreement between 2Q- and 3Q-derived order parameters in Figure 3d−f thus argues strongly that robust measures of dynamics can be obtained from the 3Q experiment presented in Figure 2 as well. As a further illustration, a linear correlation plot of S^2_{axis} values obtained from analyses of a 3Q data set (x-axis) and ^{2}H spin relaxation rates using [$^{13}CH_2D$]-labeled Leu$^{\delta}$ and Val$^{\gamma}$ methyl groups (y-axis) of ubiquitin (10 °C) is presented in Figure 4a, while the correlation for Ile$^{\delta 1}$ methyls of MSG ($^{13}CHD_2$ isotopomers are measured in the ^{2}H experiments[23,28]) is illustrated in Figure 4b. Very good correlations are obtained in both cases with Pearson correlation coefficients $R > 0.98$.

Concluding Remarks. A 3Q-based pulse scheme has been presented for quantifying methyl axis order parameters in highly deuterated, methyl-protonated proteins. Remarkably, the inherent sensitivity of the 3Q experiment exceeds that of the 2Q version by 50%. The origin of the sensitivity gain is explained, and the improved sensitivity of the experiment is subsequently demonstrated through measurements on a number of different protein systems, ranging from ~10 to 360 kDa in molecular mass. Excellent correlations between extracted methyl S^2_{axis} values from 3Q and 2Q data sets and from 3Q and ^{2}H spin relaxation measurements have been obtained, establishing the utility of the approach. The methodology presented further increases the scope of methyl groups as probes of dynamics in proteins, including systems with high molecular weights that have traditionally been challenging to study quantitatively by solution NMR spectroscopy.

AUTHOR INFORMATION

Corresponding Author

*Address: Biomolecular Sci. Bldg./CBSO, Department of Chemistry and Biochemistry, University of Maryland, College Park, Maryland 20742 USA. E-mail: vitali@umd.edu. Tel: +1-301-4051504. Fax: +1-301-3140386.

ACKNOWLEDGMENT

The authors thank Drs. Daoning Zhang and Chenyun Guo (University of Maryland) for samples of ubiquitin and MSG, and Prof. Voula Kanelis (University of Toronto) and Dr. Remco Sprangers (Max Planck Institute for Developmental Biology, Tübingen, Germany) for preparation of samples of Protein L and $\alpha_7\alpha_7$, respectively. This work was supported by a grant from the Canadian Institutes of Health Research. L.E.K. holds a Canada Research Chair in Biochemistry. V.T. would like to dedicate this paper to his coauthor and mentor Professor Lewis E. Kay on the occasion of his 50th birthday.

REFERENCES

(1) Metzler, W. J.; Wittekind, M.; Goldfarb, V.; Mueller, L.; Farmer, B. T. *J. Am. Chem. Soc.* **1996**, *118*, 6800.
(2) Gardner, K. H.; Rosen, M. K.; Kay, L. E. *Biochemistry* **1997**, *36*, 1389.
(3) Sprangers, R.; Velyvis, A.; Kay, L. E. *Nat. Methods* **2007**, *4*, 697.
(4) Ruschak, A. M.; Kay, L. E. *J. Biomol. NMR* **2010**, *46*, 75.
(5) Tang, Y.; Schneider, W. M.; Shen, Y.; Raman, S.; Inouye, M.; Baker, D.; Roth, M. J.; Montelione, G. T. *J. Struct. Funct. Genomics* **2010**, *11*, 223.
(6) Sheppard, D.; Sprangers, R.; Tugarinov, V. *Prog. Nucl. Magn. Reson. Spectrosc.* **2010**, *56*, 1.
(7) Richarz, R.; Nagayama, K.; Wüthrich, K. *Biochemistry* **1980**, *19*, 5189.
(8) Wittebort, R. J.; Rothgeb, T. M.; Szabo, A.; Gurd, F. R. *Proc. Natl. Acad. Sci. U.S.A.* **1979**, *76*, 1059.
(9) Henry, G. D.; Weiner, J. H.; Sykes, B. D. *Biochemistry* **1986**, *25*, 590.
(10) Bax, A. *Two-Dimensional Nuclear Magnetic Resonance in Liquids*; Hingham: Boston, MA, 1982.
(11) Ernst, R. R.; Bodenhausen, G.; Wokaun, A. *Principles of Nuclear Magnetic Resonance in One and Two Dimensions*; Oxford University Press: Oxford, 1987.
(12) Clore, G. M.; Gronenborn, A. M. *Science* **1991**, *252*, 1390.
(13) Wagner, G.; Thanabal, V.; Stockman, B. J.; Peng, J. W.; Nirmala, N. R.; Hyberts, S. G.; Goldberg, M. S.; Detlefsen, D. J.; Clubb, R. T.; Adler, M. *Biopolymers* **1992**, *32*, 381.
(14) Bax, A. *Curr. Opin. Struct. Biol.* **1994**, *4*, 738.
(15) Goto, N. K.; Kay, L. E. *Curr. Opin. Struct. Biol.* **2000**, *10*, 585.
(16) Tugarinov, V.; Kanelis, V.; Kay, L. E. *Nat. Protoc.* **2006**, *1*, 749.
(17) Kainosho, M.; Torizawa, T.; Iwashita, Y.; Terauchi, T.; Mei Ono, A.; Guntert, P. *Nature* **2006**, *440*, 52.
(18) Tugarinov, V.; Hwang, P. M.; Kay, L. E. *Annu. Rev. Biochem.* **2004**, *73*, 107.

(19) Kay, L. E. *J. Magn. Reson.* **2011**, *210*, 159.
(20) Kay, L. E. *J. Magn. Reson.* **2005**, *173*, 193.
(21) Muhandiram, D. R.; Yamazaki, T.; Sykes, B. D.; Kay, L. E. *J. Am. Chem. Soc.* **1995**, *117*, 11536.
(22) Millet, O.; Muhandiram, D. R.; Skrynnikov, N. R.; Kay, L. E. *J. Am. Chem. Soc.* **2002**, *124*, 6439.
(23) Tugarinov, V.; Ollerenshaw, J. E.; Kay, L. E. *J. Am. Chem. Soc.* **2005**, *127*, 8214.
(24) Tugarinov, V.; Kay, L. E. *J. Am. Chem. Soc.* **2006**, *128*, 12484.
(25) Yang, D.; Kay, L. E. *J. Magn. Reson., Ser. B* **1996**, *110*, 213.
(26) Ishima, R.; Louis, J. M.; Torchia, D. A. *J. Am. Chem. Soc.* **1999**, *121*, 11589.
(27) Ishima, R.; Petkova, A. P.; Louis, J. M.; Torchia, D. A. *J. Am. Chem. Soc.* **2001**, *123*, 6164.
(28) Tugarinov, V.; Kay, L. E. *Biochemistry* **2005**, *44*, 15970.
(29) Sprangers, R.; Kay, L. E. *Nature* **2007**, *445*, 618.
(30) Godoy-Ruiz, R.; Guo, C.; Tugarinov, V. *J. Am. Chem. Soc.* **2010**, *132*, 18340.
(31) Kay, L. E.; Torchia, D. A. *J. Magn. Reson.* **1991**, *95*, 536.
(32) Kay, L. E.; Bull, T. E.; Nicholson, L. K.; Griesinger, C.; Schwalbe, H.; Bax, A.; Torchia, D. A. *J. Magn. Reson.* **1992**, *100*, 538.
(33) Werbelow, L. G.; Grant, D. M. *Adv. Magn. Reson.* **1977**, *9*, 189.
(34) Vold, R. R.; Vold, R. L. *J. Chem. Phys.* **1976**, *64*, 320.
(35) Tugarinov, V.; Kay, L. E. *ChemBioChem* **2005**, *6*, 1567.
(36) Tugarinov, V.; Kay, L. E. *J. Am. Chem. Soc.* **2006**, *128*, 7299.
(37) Tugarinov, V.; Sprangers, R.; Kay, L. E. *J. Am. Chem. Soc.* **2007**, *129*, 1743.
(38) Muller, N.; Bodenhausen, G.; Ernst, R. R. *J. Magn. Reson.* **1987**, *75*, 297.
(39) Kay, L. E.; Prestegard, J. H. *J. Am. Chem. Soc.* **1987**, *109*, 3829.
(40) Gelis, I.; Bonvin, A. M.; Keramisanou, D.; Koukaki, M.; Gouridis, G.; Karamanou, S.; Economou, A.; Kalodimos, C. G. *Cell* **2007**, *131*, 756.
(41) Amero, C.; Schanda, P.; Durá, M. A.; Ayala, I.; Marion, D.; Franzetti, B.; Brutscher, B.; Boisbouvier, J. *J. Am. Chem. Soc.* **2009**, *131*, 3448.
(42) Ruschak, A. M.; Religa, T. L.; Breuer, S.; Witt, S.; Kay, L. E. *Nature* **2010**, *467*, 868.
(43) Religa, T. L.; Sprangers, R.; Kay, L. E. *Science* **2010**, *328*, 98.
(44) Cavanagh, J.; Fairbrother, W. J.; Palmer, A. G.; Rance, M.; Skelton, N. J. *Protein NMR Spectroscopy*; Elsevier Academic Press: Burlington, MA, 2007.
(45) Howard, B. R.; Endrizzi, J. A.; Remington, S. J. *Biochemistry* **2000**, *39*, 3156.
(46) Mittermaier, A.; Kay, L. E. *J. Am. Chem. Soc.* **2001**, *123*, 6892.
(47) Guo, C.; Zhang, D.; Tugarinov, V. *J. Am. Chem. Soc.* **2008**, *130*, 10872.
(48) Tugarinov, V.; Hwang, P. M.; Ollerenshaw, J. E.; Kay, L. E. *J. Am. Chem. Soc.* **2003**, *125*, 10420.
(49) Tugarinov, V.; Kay, L. E. *J. Biomol. NMR* **2004**, *28*, 165.
(50) Delaglio, F.; Grzesiek, S.; Vuister, G. W.; Zhu, G.; Pfeifer, J.; Bax, A. *J. Biomol. NMR* **1995**, *6*, 277.
(51) Kamith, U.; Shriver, J. W. *J. Biol. Chem.* **1989**, *264*, 5586.
(52) Skrynnikov, N. R.; Millet, O.; Kay, L. E. *J. Am. Chem. Soc.* **2002**, *124*, 6449.
(53) Sheppard, D.; Li, D. W.; Brüschweiler, R.; Tugarinov, V. *J. Am. Chem. Soc.* **2009**, *131*, 15853.
(54) Cho, C. H.; Urquidi, J.; Singh, S.; Robinson, G. W. *J. Phys. Chem. B* **1999**, *103*, 1991.
(55) Bax, A.; Griffey, R. H.; Hawkings, B. L. *J. Magn. Reson.* **1983**, *55*, 301.
(56) Mueller, L. *J. Am. Chem. Soc.* **1979**, *101*, 4481.
(57) Sørensen, O. W. *Prog. Nucl. Magn. Reson. Spectrosc.* **1989**, *21*, 503.
(58) Eliav, U.; Navon, G. *J. Chem. Phys.* **1991**, *95*, 7114.
(59) Shaka, A. J.; Keeler, T.; Fenkiel, T.; Freeman, R. *J. Magn. Reson.* **1983**, *52*, 335.
(60) Marion, D.; Ikura, M.; Tschudin, R.; Bax, A. *J. Magn. Reson.* **1989**, *85*, 393.